ELSEVIER

Chemical Engineering Journal 131 (2007) 1–13

Chemical Engineering Journal

www.elsevier.com/locate/cej

Hydrodynamics of liquid–liquid slug flow capillary microreactor: Flow regimes, slug size and pressure drop

Madhvanand N. Kashid*, David W. Agar

Institute of Reaction Engineering, University of Dortmund, Emil-Figge-Str. 66, 44227 Dortmund, Germany

Received 8 November 2005; received in revised form 21 November 2006; accepted 27 November 2006

Abstract

The use of liquid–liquid slug flow in the capillary microreactor is a promising technique for intensifying heat and mass transfer in liquid–liquid reactions. Although the concept has so far been exploited without much reference to the detailed hydrodynamics involved, these are nevertheless inherently crucial to its potential for providing well-defined reaction conditions and identifying asymptotic performance limits and thus a worthwhile subject for more rigorous analysis. In this work, the effect of various operating conditions on the flow regimes, slug size, interfacial area and pressure drop has been investigated. Experiments were carried out to determine these parameters using different Y-junction mixing elements with various downstream capillaries. The pressure drop was measured across the Y-shaped mixing element and along the length of the downstream capillaries. Since the slug flow is comprised of alternating segments of two immiscible phases, the experimentally measured pressure drop along the length of the downstream capillary was compared with a simplified theoretical prediction based on capillary pressure and hydrodynamic pressure drop of the two individual phases. As the comparison showed considerable discrepancies, the model was modified to include the formation of a thin wall film by one of the phases. The pressure drop model taking the presence of a thin film of the organic phase into account is found to be in good agreement with experimental results.

The power required for generating interfacial area was ascertained from the pressure losses over the Y-junction. The results of interfacial area and power requirement calculations indicate that the slug flow capillary microreactor is far superior to conventional equipment in terms of the specific energy, power input per unit interfacial area generated.

Keywords: Hydrodynamics; Liquid–liquid slug flow; Slug size; Interfacial area; Pressure drop; Wall film

1. Introduction

The liquid–liquid slug flow capillary microreactor has been shown to be a useful instrument for the elucidation and enhancement of fast heat and mass transfer limited reactions [1,2]. A key feature of this type of microreactor is the ability to manipulate the two principle transport mechanisms: convection within the individual slug of each liquid phase and interfacial diffusion between adjacent slugs of different phases. The stable well-defined flow patterns and uniform interfacial areas permit a precise tuning of the mass transfer processes and make an a priori prediction of mass transfer coefficients feasible. The high rates of heat transfer achieved make it possible to impose a given temperature profile along the reactor length providing additional insights into the behaviour of the reaction and indicating the asymptotic performance which can be attained. The alternative suspended drop reactor offers fewer degrees of operational freedom and precludes detailed analytical monitoring over the course of reaction. Three fundamental operational parameters characterise the slug flow capillary microreactor: the pressure drop, the mass transfer rates and the residence time distributions.

The mass transfer behaviour depends on the slug geometry and circulation patterns, which vary with the physical properties of liquids as well as with operating parameters such as flow rates, and mixing element (Y-junction) geometry and the capillary dimensions used. Burns and Ramshaw [1] have obtained mass transfer data for the extraction of acetic acid from kerosene slugs in a glass chip-based reactor and explained the performance of the system in terms of the prevailing slug lengths. Furthermore, Dummann et al. [2] studied the slug size distribution by measuring the dimensions of individual slug samples and calculating the corresponding slug volumes for a biphasic

* Corresponding author. Tel.: +49 231 755 3134; fax: +49 231 755 2698.
E-mail address: kashid@bci.uni-dortmund.de (M.N. Kashid).

1385-8947/$ – see front matter © 2006 Elsevier B.V. All rights reserved.
doi:10.1016/j.cej.2006.11.020

Nomenclature

a	specific interfacial area (m^2/m^3)
A	cross-sectional area of the microreactor capillary (m^2)
ID	internal diameter of capillary (m)
Ca	Capillary number
h	Film thickness (m)
l	length of the slug (m)
L	length of the microreactor (m)
P	pressure (kPa)
Q	volumetric flow rate (m^3/s)
r	radius of capillary (m)
V	slug flow velocity (m/s)

Greek letters

ΔP	pressure drop (kPa)
α	water phase fraction
γ	interfacial surface tension (N/m)
μ	viscosity (Pa s)
θ	contact angle

Subscripts

av	average
C	capillary
CH	cyclohexane
f	film or film region
H	hydrodynamic
s	slug
U	slug unit
W	water

nitration reaction. They reported that the distribution of the slug size for the organic phase deviates only around 5% from the mean value. The slug geometry not only defines the interfacial area but also the intensity of internal circulation which arises due to shear between slug axis and capillary wall. In our previous study concerning a simplified analysis of internal circulations using CFD simulations for different slug lengths of aqueous and organic slugs, we demonstrated that well-defined internal circulations arise in slugs having lengths greater than their diameters (for details, see [3]). This regime of slug flow, which maximises the interfacial area and internal circulations within individual slug is not feasible under all operating conditions making it an interesting topic for investigation.

Another important consideration besides the enhancement of interfacial area and intensification of internal circulations is the amount of energy required to achieve it—also a parameter of practical relevance as a benchmark for technical reactors. A few studies have been published on the experimental determination and modelling of pressure drops in two phase gas–liquid flows in microchannels (e.g., [4,5]). However, there is very little work, mostly carried out by physicists, on the pressure drop for biphasic liquid–liquid flow in capillaries. The pressure drops in such systems have generally been interpreted in terms of two contributions: the pressure drop due to the individual phases (hydrodynamic pressure drop) and the pressure drop due to the capillary effects (capillary pressure) (e.g., [6,7] and the references cited therein).

In the present work, systematic studies on slug length and pressure drop have been carried out on the chemically inert water–cyclohexane system. The existence of well-defined slug flow was investigated for different Y-junction mixing elements and various downstream capillaries. The slug length and contact angles were measured using a snapshot approach under similar operating conditions and corresponding interfacial area was determined. In addition to this, the pressure drop across different Y-junction mixing elements and along the length of each capillary was measured at various flow velocities. The simplified theory was employed to calculate the pressure drop along the length of capillary and the predications were compared with experimental results. Based on the contribution of the Y-junction to the overall pressure drop, the power requirement was estimated and compared with values for conventional equipment.

2. Experimental set-up

A schematic flowsheet of the experimental set-up for slug length and pressure drop measurement is depicted in Fig. 1. It consists of two computer-controlled continuously operating high precision piston pumps to feed two immiscible liquids smoothly to a PTFE Y-junction mixing element with an angle of 120° between two inlet lines. An important characteristic of the Y-junction is that all three of its branches have equal dimensions. A transparent PTFE capillary, the 'capillary microreactor', is attached directly downstream of the Y-junction. The photographic system comprises a commercial camera (Olympus E-20P with Macro extension lens WCON-08B) fitted at a length of 0.5 m downstream of the mixing element and a light source (2000 W). The transducers (range, 0–1 bar) to measure pressure drop were mounted at different locations including one on each inlet line at a distance of 0.25 m upstream of the Y-junction, one at Y-junction and one at a distance 0.5 m downstream of the Y-junction. Further, the positions of transducers were changed in order to measure the pressure gradient along the length of the

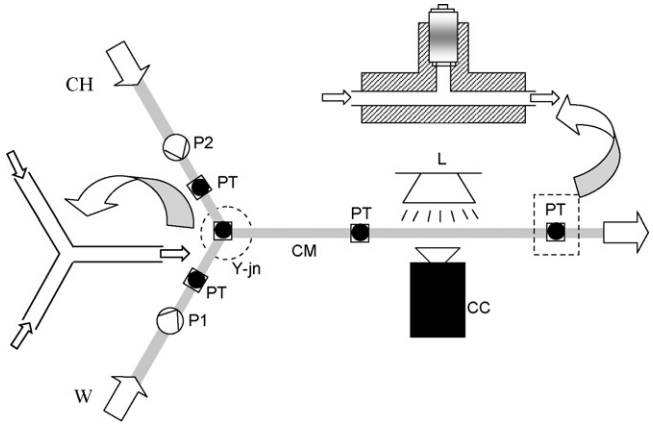

Fig. 1. Schematic of experimental set-up. P1, P2: piston pumps; PT: pressure transducer; Y-jn: Y-junction; CM: capillary microreactor; L: light; CC: camera; W: water; CH: cyclohexane.

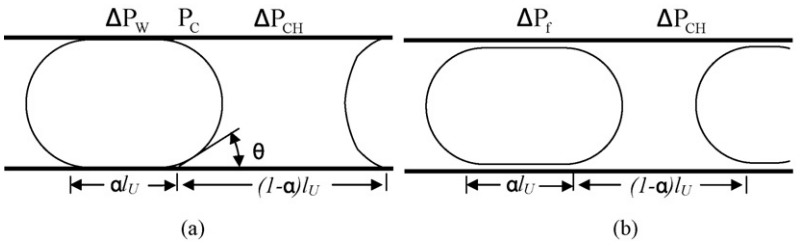

Fig. 2. Pressure drop along single slug unit: (a) without film and (b) with film.

downstream capillary. The transducers were attached to the capillaries with the help of PTFE T-junctions with the construction illustrated, while the transducer at Y-junction is attached to a similar port at the Y-junction.

Experiments were carried out for different combinations of the Y-junctions having an internal diameter of 0.25–1 mm and with capillaries of internal diameters ranging from 0.25 to 1 mm. Water was used as an aqueous phase while cyclohexane constituted the organic phase. The two liquids were introduced at constant pressures and the volumetric flow rates were controlled precisely. The camera was adjusted so as to capture approximately 10 slugs in an exposure. The experiments were carried out with equal and unequal inlet flow rate combinations for each phase in the range of 5–200 ml/h for all capillaries. Four snapshots were taken under each set of flow conditions and the experiments were repeated twice in order to confirm the reproducibility of snapshots and pressure drop measurements. The snapshots for the contact angle measurement were taken under both flow and stationary conditions.

The snapshots were analysed using the Adobe Photoshop® and Image Tool software (developed by University of Texas Health Science Centre San Antonio). The lengths were calibrated using the diameter of the slug and defined along the central axis of the slug. For a given snapshot maximum and minimum slug unit (i.e., a pair of aqueous and organic slugs) lengths and individual slug lengths were established, from which the average lengths, average slug size of each phase, interfacial area and standard deviations were then calculated. The three phase contact angle was also ascertained using the above-mentioned Image Tool software.

3. Pressure drop

There are two basic contributions to the overall pressure drop in the liquid–liquid slug flow capillary microreactor: pressure drop across the mixing element and pressure drop along the length of the capillary. The present theoretical work considers only the latter, which should be, in principle, obtainable from addition of the hydrodynamic pressure drop of the individual phases and the pressure drop due to capillary phenomena. However, in many of the studies and some of our own laboratory experiments, it was revealed that the cyclohexane forms a thin organic wall film due to the superior wetting properties of cyclohexane on the capillary material (PTFE). So in the present work both cases, i.e., without and with film, are considered for the theoretical prediction of pressure drop.

3.1. Pressure drop—without film

If we consider a single flow unit as shown in Fig. 2a, the overall pressure drop along its length can be written as:

$$\Delta P_{\mathrm{U}} = \Delta P_{\mathrm{H}} + P_{\mathrm{C}} = \Delta P_{\mathrm{W}} + \Delta P_{\mathrm{CH}} + P_{\mathrm{C}} \tag{1}$$

The hydrodynamic pressure drop can be calculated from the Hagen–Poiseuille equation, while the capillary pressure is obtained from the Young–Laplace equation for a cylindrical tube [7] given by the following equations:

$$\Delta P_{\mathrm{W}} = \frac{8\mu_{\mathrm{W}} V\alpha l_{\mathrm{U}}}{r^2}; \qquad \Delta P_{\mathrm{CH}} = \frac{8\mu_{\mathrm{CH}} V(1-\alpha) l_{\mathrm{U}}}{r^2};$$

$$P_{\mathrm{C}} = \frac{2\gamma}{r}\cos\theta \tag{2}$$

where $V = (Q_{\mathrm{W}} + Q_{\mathrm{CH}})/A$.

Assuming a constant dynamic contact angle and slug lengths with equal number of slugs of water and cyclohexane under similar operating conditions and neglecting end effects, the equation for pressure drop across the length of the capillary becomes:

$$\Delta P = \frac{L}{l_{\mathrm{U}}}(\Delta P_{\mathrm{W}} + \Delta P_{\mathrm{CH}}) + \frac{2L - l_{\mathrm{U}}}{l_{\mathrm{U}}} P_{\mathrm{C}} \tag{3}$$

3.2. Pressure drop—with film

When the slugs move through the capillary, depending on the physical properties of the liquids and capillary wall, one of the liquids often forms the film. The presence of a film and its effect on the circulatory flow within the slug is explained in detail in Ref. [3]. During the present study of pressure drop without considering a film, discrepancies were observed (which are described in the results and discussion section) and therefore, as one possible explanation, it was decided to analyse the pressure drop with film formation. Since the organic liquid has affinity towards the PTFE material, cyclohexane was assumed to form the wall film and water flows as enclosed slugs. In this situation, the film has a major influence compared to slugless flow (only cyclohexane flow) and therefore, for theoretical predictions, it is considered that the pressure drop along the length of the capillary is due to this region only.

A theoretical model for pressure drop in the pipeline flow of capsule is given in Ref. [8] which relates the pressure drop in the capsule region to that for single phase flow. According to his predictions, the pressure drop along the length of the film can

be given by the following equation,

$$\left(\frac{\Delta P}{L}\right)_{\mathrm{f}} = \left(\frac{1}{1-k^4}\right)\left(\frac{\Delta P}{L}\right)_{\mathrm{CH}} \tag{4}$$

where $k = (R-h)/R$.

However, in his predictions it was assumed that the capsules follow each other sufficiently closely for the fluid between the capsules to be considered as part of the capsule stream. In the present case of liquid–liquid slug flow this assumption is usually not valid and will only apply when the water slugs have lengths several times greater than the cyclohexane slugs. The slug which forms the film may, however, be longer depending on the inlet flow ratio for both phases. It is therefore necessary to consider the phase fraction of both the liquids to calculate the pressure drop for a given length of the liquid–liquid slug flow capillary microreactor. In addition, the film thickness is very small compared to the radius of slug, which justifies the assumption that the length of the film region for a given length of capillary is nothing more than the water phase fraction times the total length. The pressure drop along the film region in the given capillary/pipe length can thus be written as:

$$\left(\frac{\Delta P}{\alpha L}\right)_{\mathrm{f}} = \left(\frac{1}{1-k^4}\right)\left(\frac{\Delta P}{\alpha L}\right)_{\mathrm{CH}} \tag{5}$$

According to Hagen–poiseuille equation, the single phase pressure drop per unit length is same for all lengths, i.e.,

$$\left(\frac{\Delta P}{\alpha L}\right)_{\mathrm{CH}} = \left(\frac{\Delta P}{L}\right)_{\mathrm{CH}} \tag{6}$$

Therefore, the overall pressure drop, which is due to film region only, per unit capillary length can be written as:

$$\frac{\Delta P}{L} = \left(\frac{\alpha}{1-k^4}\right)\left(\frac{\Delta P}{L}\right)_{\mathrm{CH}} \tag{7}$$

To calculate the pressure drop using the above equation, the film thickness is crucial. It can be estimated using Bretherton's law, as a function of capillary number, given by the following equation [9].

$$h = 1.34RCa^{2/3} = 1.34R\left(\frac{\mu_{\mathrm{CH}} V_{\mathrm{s}}}{\sigma_{\mathrm{CH}}}\right)^{2/3} \tag{8}$$

In the definition of capillary number the velocity used is called the velocity of film deposition and is considered to be the velocity of the slug, which is slightly greater than the average flow velocity. In analogy to the theoretical predictions of Charles [8] for pipeline flow of capsules, the slug flow and average flow velocity can be related by:

$$V_{\mathrm{s}} = \left(\frac{2}{1+k^2}\right) V_{\mathrm{av}} \tag{9}$$

Substituting h from Eq. (5) in (8) and V_{s} from (9), the Eq. (8) will yield a non-linear equation which can be solved iteratively.

4. Results and discussion

4.1. Flow regime

4.1.1. Flow regime—the basic structure

When two immiscible liquids are introduced into the Y-junction, one liquid initially flows downstream through the junction, while the other penetrates over to the opposite side of the junction, this mutual displacement process generates the characteristic alternating slug flow structure which has been confirmed qualitatively by CFD simulations (Kashid et al. [10]). In order to distinguish the two phases, the water phase was stained with a blue dye (brilliant blue) to appear darker than the colourless cyclohexane. The experimental results show that the water forms convex shaped slug while cyclohexane exhibits a concave geometry, as would be expected with the hydrophobic PTFE wall material. The exact form of the slug depends on the inlet flow ratios and the capillary and Y-junction dimensions. The experimental snapshots of prevailing flow regime of alternating two phase flow structures are shown in Fig. 3. One can easily recognise three distinct flow regimes, well-defined slug flow, drop flow and deformed interface flow. This characterisation refers to the behaviour of the water slug during flow and can be explained as follows.

Slug flow: In this flow regime, the slugs of both phases have a length greater than their diameter. This flow pattern occurs at relatively low and approximately equal flow rates of both liquids. There is no coalescence or break-up of the slugs and stable flow prevails as a consequence.

Drop flow: In this regime, the water flows as small drops entrained in the organic phase due to the low water to cyclohexane ratio, while cyclohexane forms extended slugs, of a length which increases with increasing cyclohexane flow rate.

Deformed interface flow: In the case of deformed slug flow, at high water to cyclohexane ratio ($Q_{\mathrm{W}}/Q_{\mathrm{CH}}$), water forms long slugs while cyclohexane is present as small droplets. This regime is less stable, because with increasing Q_{W} at constant Q_{CH}, the deformation of hemispherical caps of water slug becomes more pronounced and they tend to form bridges between adjacent water slugs, which may lead to the formation of still larger slugs by coalescence.

4.1.2. Effect of capillary and Y-junction dimensions

The effect of equal values of the capillary and Y-junction internal diameter on the flow regimes observed is presented in Fig. 4. The individual grid points in this figure correspond to the inlet volumetric flow rates of the two liquids into the Y-junction used for the experiments, while the bounded region indicates the conditions under which well-defined slug flow arises. As can be observed, the well-defined slug flow behaviour is observed at relatively low and approximately equal flow rates and its extent varies with the capillary dimensions. In the case of a small capillary (ID = 0.5 mm), slug flow is observed for the same maximum flow rates of 70 ml/h for both liquids and beyond this point the flow was found to be completely unstable. However, for the larger capillaries (ID = 0.75 and 1 mm), the well-defined uniform slug flow was observed up to a maximum flow of 100 ml/h

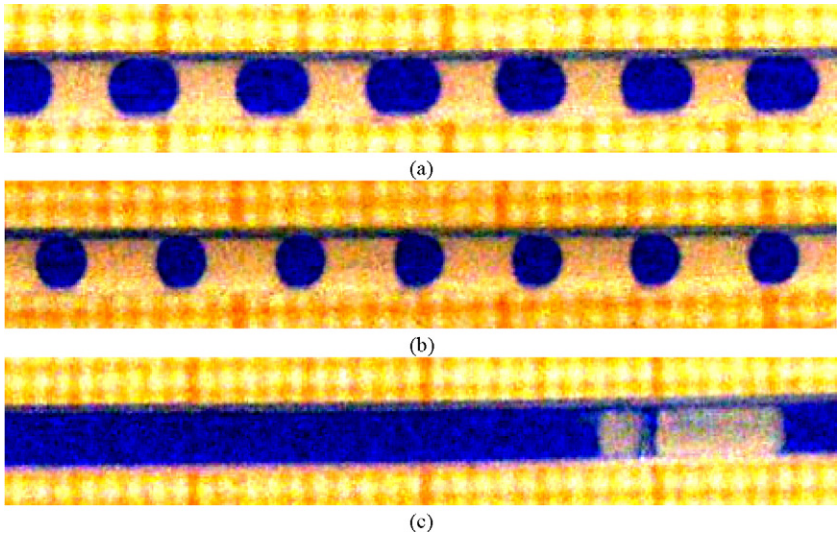

Fig. 3. Observed flow regimes in the capillary microreactor (Y-junction ID = 1 mm, capillary ID = 1 mm). (a) Slug flow, (b) drop flow and (c) deformed interface flow.

which is the maximum flow rate for both liquids in the present study. Other investigations of the flow regime at unequal flow rates of both phases revealed that the transition of the slug flow to deformed interface flow and drop flow varies with the dimensions. The transition of slug flow to deformed interface flow occurs approximately in the Q_W/Q_{CH} range of 2.5–5, while the transition of slug flow to drop flow occurs in the Q_{CH}/Q_W range of 3–6. In the case of small capillary dimensions (ID = 0.5 mm), the transition to deformed interface flow takes place at Q_W/Q_{CH} equal to 2.5 while drop flow arises at the ratio of Q_{CH}/Q_W equal to 3 or higher. The difference between the ratios for the transition from slug flow to deformed interface flow and drop flow is thought to be due to the hemispherical caps of the water slug. The transition boundary broadens with increase in the capillary internal diameter.

In order to study the effect of capillary and Y-junction dimensions on the flow regime separately, experiments were carried out for different capillaries with constant Y-junction dimensions and vice a versa. Fig. 5 depicts the effect of different capillary dimensions on the flow regime for the same Y-junction. This figure is qualitatively similar to Fig. 4 and shows no significant difference between constant and varying dimensions of the Y-junction. However, the different Y-junction for the same capillary diameter exhibits a considerable effect on the flow regime. Fig. 6 depicts the effect of Y-junction dimensions (ID = 0.25–1 mm) on the flow regime for constant capillary internal diameter (0.75 mm). It shows that the well-defined slug flow occurs at all flow rates. In the case of a fine bore Y-junction (ID = 0.25 mm), the transition from slug flow to deformed interface flow occurs at a Q_W/Q_{CH} equal to 2.5 and slug flow to drop flow at a Q_{CH}/Q_W of approximately 3. This transition boundary

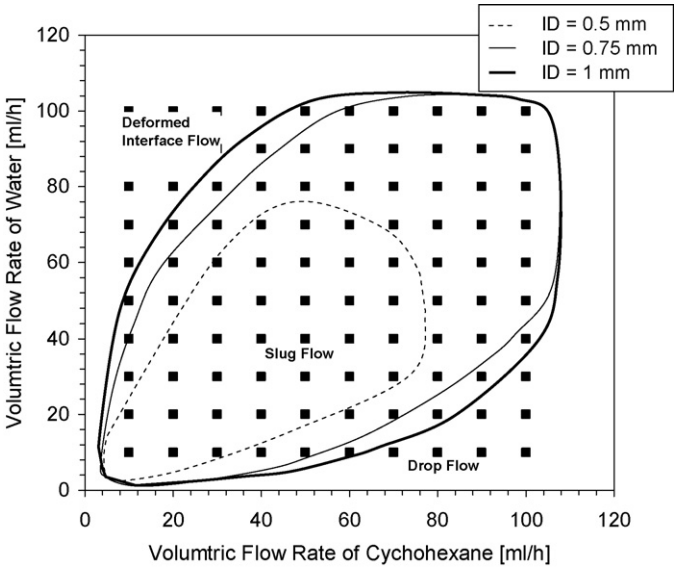

Fig. 4. Observed flow regimes for equal capillary and Y-junction internal diameters.

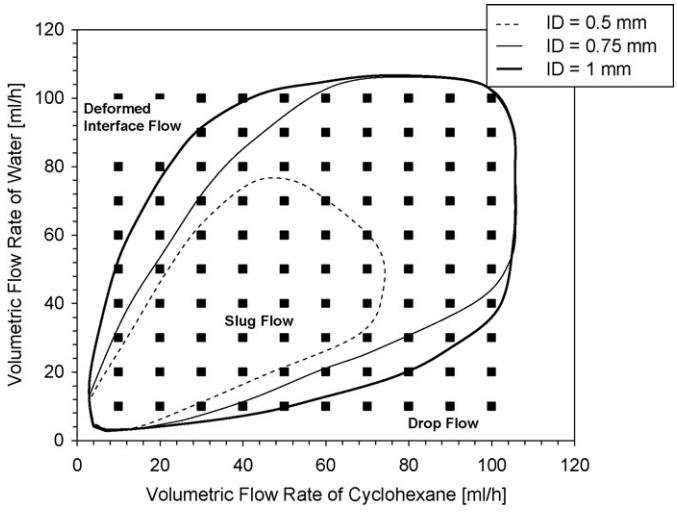

Fig. 5. Observed flow regimes for different capillaries at same Y-junction diameter (Y-junction ID = 0.5 mm).

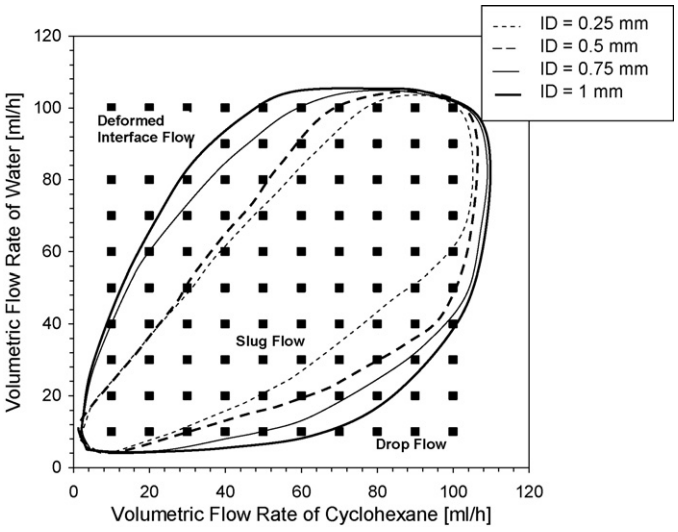

Fig. 6. Observed flow regimes for various Y-junctions for same capillary (ID = 0.75).

of the slug flow to the drop flow and deformed interface flow broadens with increasing Y-junction ID for same capillary bore.

4.2. Slug size measurement

As discussed in the above section, the well-defined slug flow exists over a wide operating window, which guarantees a well-defined interfacial area for mass transfer. This information alone, of course, is not enough for a priori prediction of mass transfer and therefore the experiments were carried out to investigate the slug size in the well-defined slug flow regime. The effects of various operating conditions on the well-defined slug flow regime are discussed below.

4.2.1. Effect of slug flow velocity

The effect of slug flow velocity at identical flow rates of both phases and at equal Y-junction and capillary ID is plotted in Fig. 7a. Although the photographic evidence suggests that the slug flow is comprised of an alternating sequence of uniform slugs, the microscopic analysis reveals that the variation in slug size is by no means negligible. As illustrated in the Fig. 7a, the slug size deviates from the mean value by 5%. An advantage of high average flow velocity is that the slug size diminishes with increasing slug flow velocity. This is due to the rapid penetration of one phase into other, which segregates the stream into a greater number of segments. One thus achieves higher specific interfacial areas and consequently increased mass transfer rates between adjacent slugs due to the decrease in the volume of individual slugs for a given flow rate.

An alternative method to augment the interfacial area is to vary the ratio of inlet flow rates. In our experiments with variable flow rate ratios, which were carried out by keeping one liquid flow rate constant and varying the other, the volume of the slug phase with constant liquid flow rate decreases and slug volume of varying flow rate increases with increase in the flow rate as depicted in Fig. 7b—a not entirely unexpected result. However, the deviation of the slug size from mean remains the same.

4.2.2. Effect of capillary diameter

In order to study the effect of the capillary internal diameter on the slug size, experiments were carried out with different capillary diameters using the same Y-junction. The average slug volume for the aqueous phase is plotted as a function of slug flow velocity for identical inlet volumetric flow rates of both liquids for different capillaries and 0.5 mm ID Y-junction in Fig. 8a. The slug size increases with an increase in the capillary ID for all slug flow velocities. As described above, for equal capillary and Y-junction ID, the slug size diminishes with increasing slug flow velocity. In the case of small differences between the capillary and Y-junction dimensions (e.g., Y-junction with 0.5 mm ID and capillary with 0.75), there is no significant difference in the trends. However, with further increase in the capillary ID, the trend of slug size with respect to flow velocity changes, which is in at variance with the results obtained for equal Y-junction and capillary ID. For a Y-junction with 0.5 mm and a capillary with 1 mm ID for instance, the slug size first increases with slug flow velocity. However, this trend is only temporary and beyond a flow velocity of 40 mm/s, the slug volume

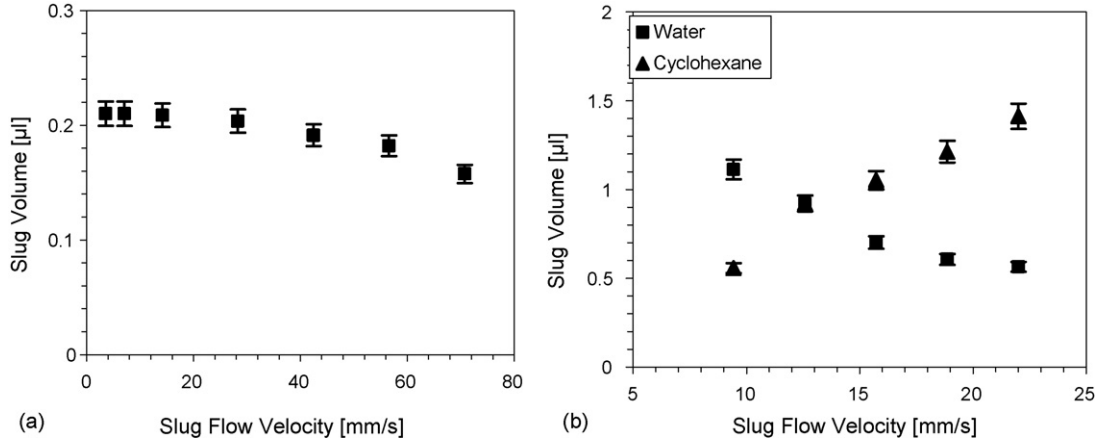

Fig. 7. Slug size as a function of slug flow velocity for similar Y-junction and capillary ID. (a) Water slug size at equal flow rate of both phases (ID = 0.5 mm) and (b) water and cyclohexane slug size at unequal flow rate of both phases (constant flow rate of water, 10 ml/h and ID = 0.75 mm).

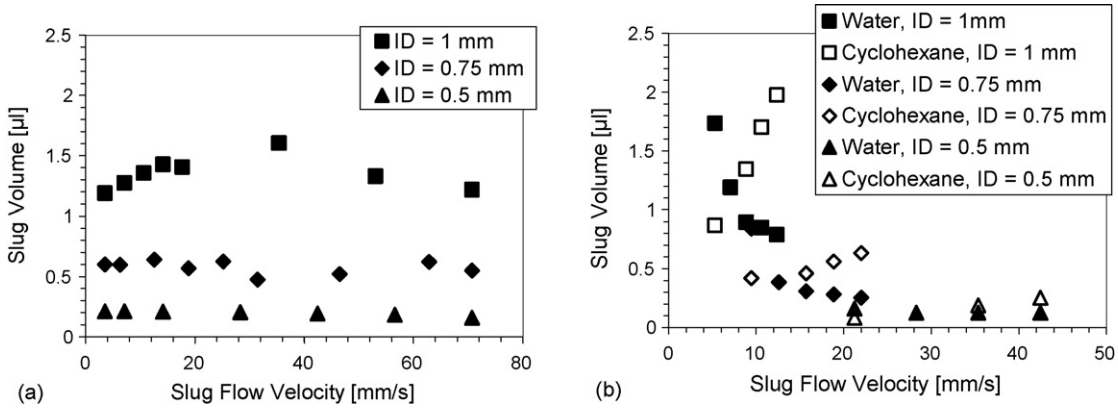

Fig. 8. Slug size for different capillary diameter for the same Y-junction diameter. (a) For equal flow of both phases (Y-junction ID = 0.5 mm) and (b) for constant flow rate of water (Y-junction ID = 0.25 mm).

diminishes. This complex behaviour of slug volume for similar inlet flow rates is probably due to the different diameters affecting slug coalescence in the vicinity of Y-junction. In addition to this, different diameters for the Y-junction and capillary lead to increased deviation of slug size from the mean value of around 10% for the configuration described. The experiments with unequal flow rates of water and cyclohexane yielded similar results for increased capillary diameters as shown in Fig. 8b.

4.2.3. Effect of Y-junction diameter

From the above discussion it is clear that the change in the capillary diameter exerts a major influence on the slug size. Similarly, a change in Y-junction ID also affects the slug size significantly. Increased Y-junction diameters yield larger slugs in comparison to smaller Y-junctions for the same capillary dimensions as shown in Fig. 9a, which depicts slug size for different Y-junctions ranging from 0.25 to 0.75 mm ID for a capillary with 0.75 mm. For all Y-junctions the slug size behaviour with respect to the flow velocity is the same, even though there is difference of 0.5 mm in capillary and Y-junction ID for the case of capillary with 0.75 mm and Y-junction with 0.25 mm ID. As expected, the same results were obtained for unequal flow rates as illustrated in Fig. 9b.

4.3. Interfacial area

The well-defined flow patterns under slug flow regime make it possible to investigate the interfacial area from the experimental snapshots by simply measuring the size of aqueous and organic slug. Just as the slug size deviated to some degree from its mean value, a similar deviation was observed in the interfacial area. From the pressure drop studies (which are discussed in the next section), it was concluded that an organic wall film is present. Two cases are therefore considered for the investigation of interfacial area: without film and with film. However, as it was difficult to visualise such a film with the resolution of our photographic equipment and the interfacial areas for the latter case were based on length of slug measured from experimental snapshots and film thickness calculated from Bretherton's law. For the case without film, only the hemispherical ends (caps) of the aqueous slug participate in the mass transfer process while in the later case, with a wall film, the whole of the aqueous slug is involved, which of course enhances the overall transfer across the interface.

The interfacial area as a function of slug flow velocity for different capillaries and Y-junctions and for equal velocities of both phases is plotted in Fig. 10. From the figure, one can appreciate that the presence of a wall film enhances mass

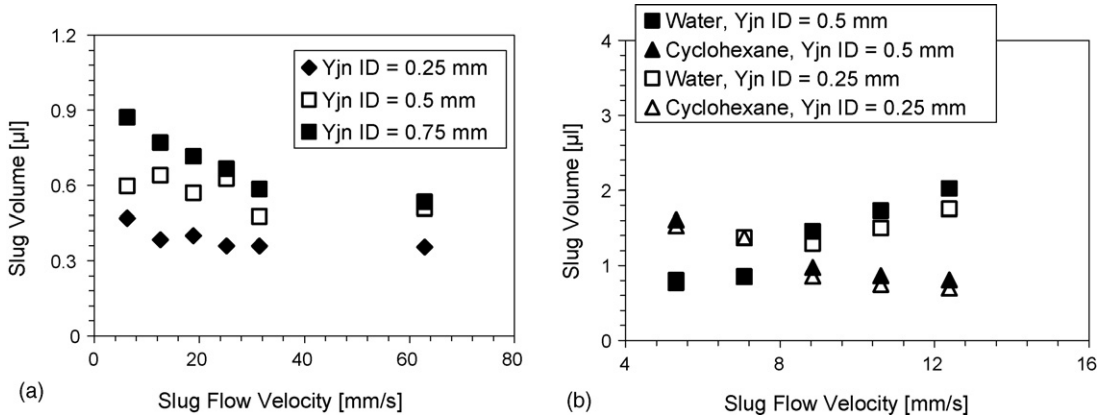

Fig. 9. Slug size for different Y-junctions using the same capillary. (a) Water slug size for equal flow rate of both phases (ID = 0.75 mm) and (b) constant water flow rate (Q_W = 10 ml/h, ID = 1 mm).

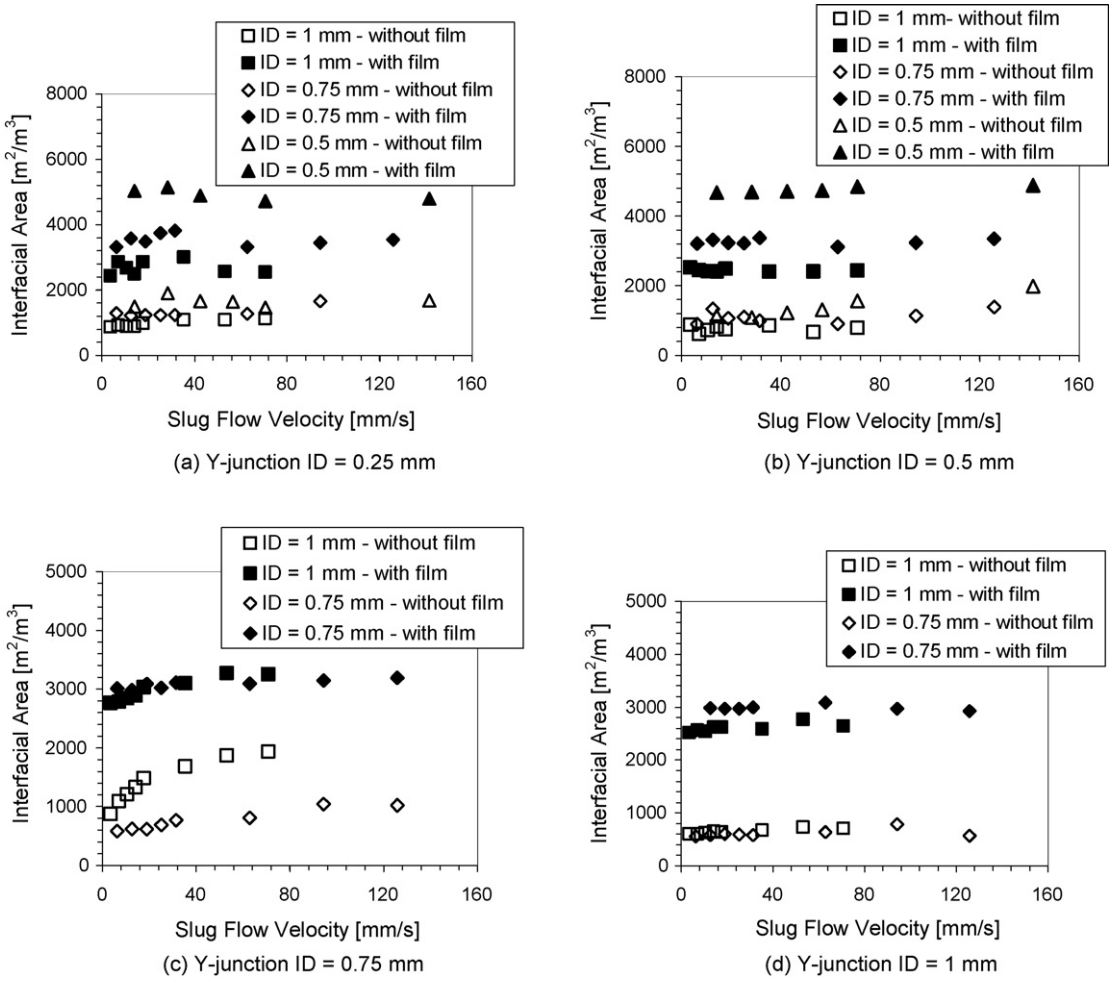

Fig. 10. Specific interfacial area for different Y-junction and capillary internal diameters. (a) Y-junction ID = 0.25 mm, (b) Y-junction ID = 0.5 mm, (c) Y-junction ID = 0.75 mm and (d) Y-junction ID = 1 mm.

transfer significantly, as increasing the interfacial area by a factor of 2–4 under all operating conditions. However, the range of interfacial area varies considerably with the capillary and Y-junction dimensions. The range of interfacial area for various operating conditions is given in Table 1 which shows that increased capillary and Y-junction dimensions reduce the interfacial area. Recently, Dehkordi [11] has investigated a novel reactor referred to as a two-impinging-jets reactor which is characterised by a small reactor volume equipped with two simple nozzles directed towards each other in which interfacial area as high as 3500 m^2/m^3 was found, which is way above the values in a mechanically agitated reactor ($a \approx 500\ m^2/m^3$). The interfacial area was established assuming mass transfer with chemical reaction for a pseudo-first order heterogeneous liquid–liquid

Table 1
Specific interfacial area for different capillaries and Y-junctions at equal and unequal flow rates of water and cyclohexane

Y-ID (mm)	ID (mm)	$Q_W = Q_{CH}$		$Q_W = 10$ ml/h		$Q_{CH} = 10$ ml/h	
		a (m^2/m^3)	a_f (m^2/m^3)	a (m^2/m^3)	a_f (m^2/m^3)	a (m^2/m^3)	a_f (m^2/m^3)
0.25	0.5	1450–1680	4700–5100	1110–1905	4550–5100	1070–1480	4700–5130
	0.75	1220–1660	3300–3800	990–1220	3570–3720	930–1220	3540–3700
	1	860–1130	2430–2310	560–920	2550–2850	610–920	2550–2850
0.5	0.5	1080–1970	4500–4800	1085–1770	3660–4690	1085–1980	3300–4600
	0.75	880–1330	3200–3330	960–1330	2520–3300	1205–1334	2782–3310
	1	620–870	2400–2510	730–1025	1860–2440	750–1380	2024–3500
0.75	0.75	870–1686	2980–3190	540–630	2190–3010	620–990	3010–3560
	1	580–1040	2760–3090	490–1090	1710–2780	960–1410	2780–3170
1	0.75	560–780	2560–3080	580–620	1970–2440	510–580	1940–3400
	1	590–780	2510–2760	550–670	1750–2380	500–690	2520–3190

reaction. The directly measured interfacial area for the slug flow capillary reactor compares favourably with the impinging jet reactor in the velocity range of 0–0.15 m/s. In addition to this, the presence of film in liquid–liquid slug flow offers 2–4 times more interfacial area under the same operating conditions. The interfacial area obtained can be manipulated precisely due to the well-defined flow pattern and one can thus regulate interfacial mass transfer.

4.4. Pressure drop

4.4.1. Pressure drop across Y-junction

The power required to provide a unit interfacial area, a parameter of practical relevance as a benchmark for technical reactors, can be calculated from the contribution of Y-junction in the overall pressure drop. Therefore, experiments were carried out to measure the pressure drop across the Y-junction. Initially, several experiments were carried out in order to identify the most suitable pressure measurement points. This was done by taking sequential videos under various operating conditions and selecting four locations including two on the inlet lines at a distance 0.25 m upstream of the Y-junction, one at the junction itself and one at a distance 0.5 m downstream for mounting pressure transducers. The pressures were measured under various operating conditions and the differences between them are referred to as $\Delta P1$, $\Delta P2$ and $\Delta P3$ as shown in Fig. 11. As with the pressure drop in a single pipe/capillary, the pressure drop increases with decrease in the internal diameter as depicted in the Fig. 11. As can be seen, the major contribution to the pressure drop during slug generation is $\Delta P3$, the pressure drop between a point on Y-junction and the point 0.5 m downstream in the capillary. The pressure drops between the inlet and Y-junction, $\Delta P1$ and $\Delta P2$, are much lower and are more or less equal to the pressure drop for single phase flow through the capillary, i.e., the Hagen–Poiseuille pressure drop.

In order to observe the effect of the Y-junction on the pressure drop for equal inlet flow velocities, the variation of pressure

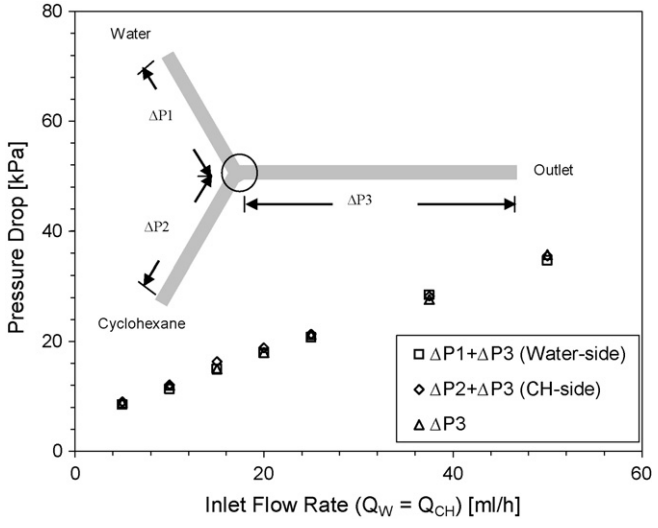

Fig. 11. Pressure drop across the Y-junction at equal flow rates of water and cyclohexane (capillary ID = Y-junction ID, 0.5 mm).

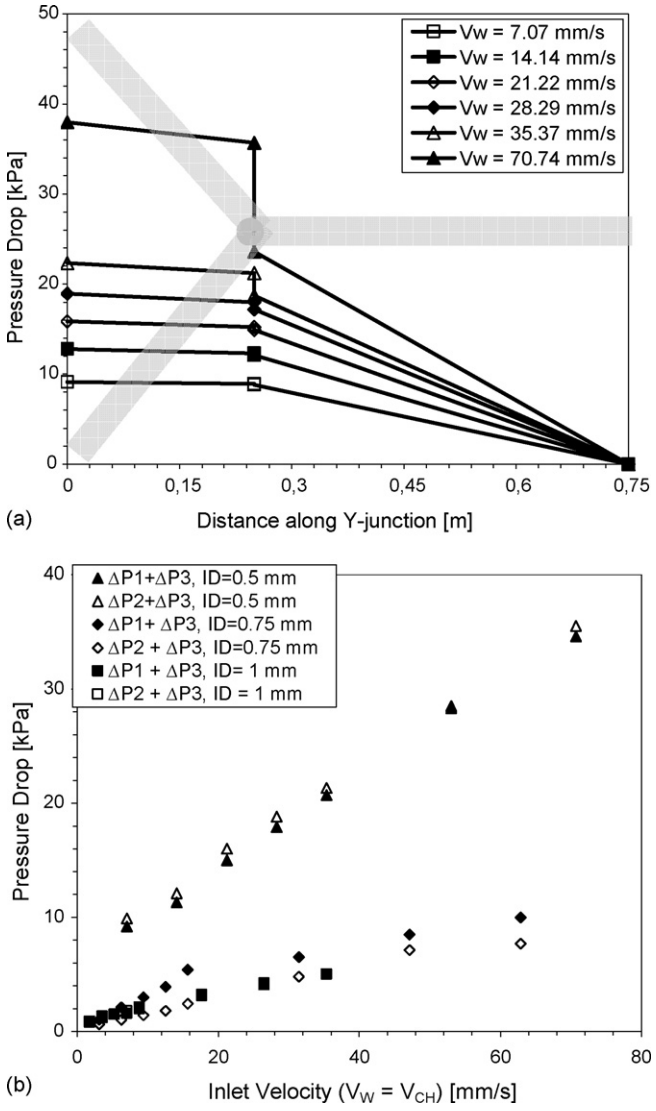

Fig. 12. Pressure drop in the vicinity of Y-junction at equal flow rates of water and cyclohexane. (a) Behaviour of pressure along the length of Y-junction and (b) pressure drop for different internal diameters.

along the length of the Y-junction and connected capillaries for equal inlet flow velocities is plotted in Fig. 12a. The pressure loss due to the Y-junction is calculated by measuring ΔP_3 and the pressure gradient along the length of the capillary (discussed below). The results show that with increasing water inlet flow velocity, up to 25 mm/s, there is negligible pressure drop while for further increases in it the losses become significant. At the transition boundary of the well-defined slug flow (the velocity beyond which the slug flow does not exist, 70 mm/s in this case), the pressure drop is about 12 kPa. Since the inlet velocity of water and cyclohexane is the same, similar pressure variations along the Y-junction were observed for different inlet velocities of cyclohexane. Further experiments were carried out to study the effect of capillary dimensions on the pressure drop across the Y-junction which was found to increase with decreasing capillary ID as shown in Fig. 12b.

As we already know, the introduction of unequal flow rates to Y-junction can affect the slug size and thus the interfacial area;

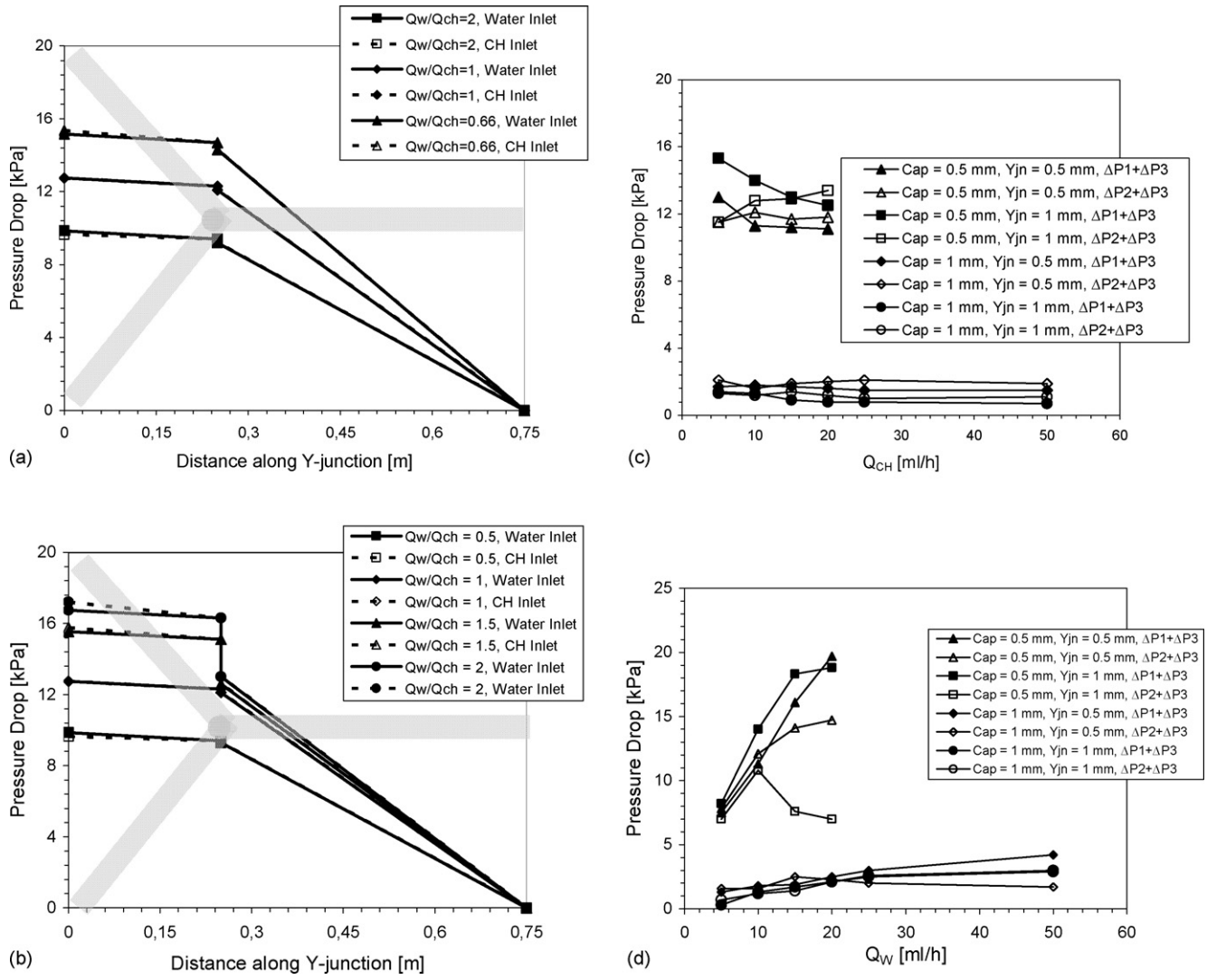

Fig. 13. Pressure drop in the vicinity of Y-junction at unequal flow rates of water and cyclohexane. (a) Behaviour of pressure along the length of Y-junction at constant water flow rate, $Q_W = 10$ ml/h, (b) pressure drop for different internal diameter at constant cyclohexane flow rate, $Q_{CH} = 10$ ml/h, (c) pressure drop for different capillary internal diameter at constant flow rate of water, $Q_W = 10$ ml/h and (d) pressure drop for different capillary internal diameter at constant flow rate of cyclohexane, $Q_{CH} = 10$ ml/h.

and such asymmetric flow conditions will be the rule rather than the exception in chemical engineering processes. Therefore the measurements were carried out across the Y-junction for unequal flow rates of water and cyclohexane, i.e., done by keeping one of the flow rates constant and varying the other. The behaviour of the pressure drop in a capillary of internal diameter 0.5 mm along the Y-junction for various inlet flow ratios is plotted in the Fig. 13a and b. As can be seen from the Fig. 13a, at constant flow rate of water, the most significant effect was observed at a flow ratio of 0.66 ($Q_{CH} = 15$ ml/h), beyond which the slug flow disappeared. The same trends were observed at constant flow rate of cyclohexane, as shown in Fig. 13b. Both figures indicate that the pressure loss contribution of the Y-junction rises with increasing total flow rate.

Further experiments were carried out under well-defined slug flow regime condition to establish the pressure drop across the junction ($\Delta P1 + \Delta P3$ and $\Delta P2 + \Delta P3$) at unequal flow rates of water and cyclohexane for both similar and dissimilar dimensions of Y-junction and three downstream capillaries. For similar internal diameter of capillary and Y-junctions, at constant flow rate of water, the water-side pressure drop ($\Delta P1 + \Delta P3$) decreases with increase in the inlet flow rate of cyclohexane, while the pressure drop on the cyclohexane side ($\Delta P2 + \Delta P3$) remains almost constant. However, in the case of dissimilar internal diameters for the capillaries and Y-junctions (e.g., capillary ID = 0.5 mm and Y-junction ID = 1 mm), the water-side pressure drop ($\Delta P1 + \Delta P3$) decreases while the cyclohexane side pressure drop rises with increasing cyclohexane flow rate at constant water flow. In the case of larger capillary ID and small Y-junction bores, there is a significant effect of cyclohexane flow velocity on the pressure drop on both sides. The trends described are significantly different in the case of a constant flow rate of cyclohexane for increasing water flow rate.

In all cases of similar and dissimilar dimensions of capillaries and Y-junctions, the pressure drop increases markedly at higher water flow rates. This behaviour of pressure drop may be due

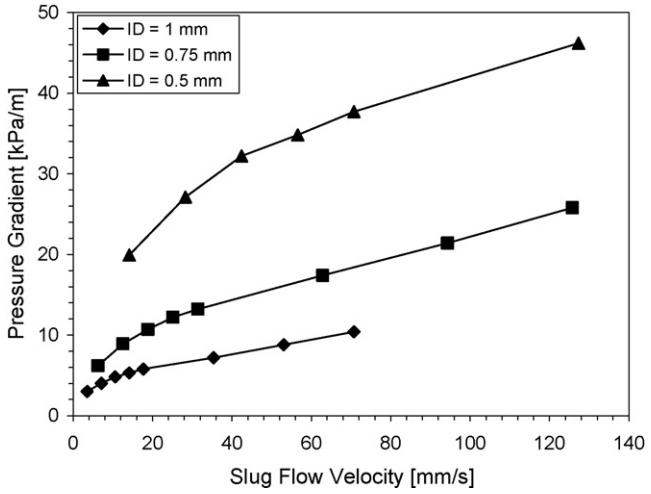

Fig. 14. Experimental pressure drop along the length of the capillary microreactor for equal flow rates of water and cyclohexane.

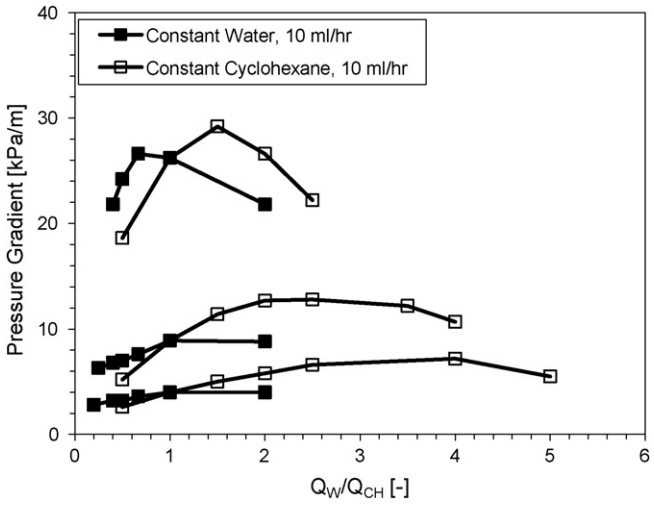

Fig. 15. Pressure gradient as a function of water to cyclohexane ratio for constant water and constant cyclohexane flow rate.

to the presence of an organic wall film in the capillary, since in the absence of film the pressure drop should be approximately equal under both sets of conditions due to the similar properties of the liquids. In the presence of a film at constant flow rate of water, the slug size decreases significantly with increasing cyclohexane flow rates thereby reducing proportionately the overall film region which thus exerts a lower shear stress and exhibits no significant effect. For constant cyclohexane flow rate on the other hand, the length of enclosed (water) slug increases with increasing water flow thus giving rise to a larger pressure drop.

4.4.2. Pressure drop along the length of capillary

4.4.2.1. Experimental. The pressure drop across a given length of the liquid–liquid slug flow capillary microreactor was measured for different slug flow velocities and inlet flow ratios for various Y-junction and capillary dimensions. Fig. 14 depicts the pressure drop behaviour observed for equal flow rates of both phases. The results show that for equal flow rates and for all capillaries, the pressure drop increases with increasing slug flow velocity and is furthermore a strong function of capillary ID as capillary effects dominate the behaviour at such small dimensions. As would be expected, the pressure drop was found to be larger for smaller capillary ID. In the experiments carried out with larger capillaries (ID = 1 mm) the pressure drop increased from the low values observed at slow flow up to a certain value and subsequently remained constant. For small capillaries (ID = 0.5 and 0.75 mm), on the other hand, the pressure drop increases further in the same velocity range.

The pressure drop for different flow ratios, which was measured keeping one of the flow rates constant, and the comparison with constant flow rates of water and cyclohexane is illustrated in Fig. 15, which shows that the pressure drop increases with an increase in the flow ratio of water to cyclohexane but the trend is reversed beyond a certain flow ratio, and subsequently decreases. As with the equal flow rate pressure drop behaviour, the capillary dimensions are decisive. Additionally an interesting phenomenon arises at constant velocities of water and cyclohexane. At low Q_W/Q_{CH} ratios, the pressure drop at constant flow rate of cyclohexane is less than at constant water flow rate and vice versa at higher Q_W/Q_{CH} flow ratio. The flow ratio corresponding to the maximum pressure drop is different for different capillary dimension and flow rates. For a constant water flow rate, it is 0.65 for the capillary with 0.5 mm ID and 1 for the capillaries with 0.75 and 1 mm ID, while for constant flow rate of cyclohexane it is 1 for the 0.5 mm ID capillary and 2 and 2.5 for 0.75 and 1 mm ID, respectively. The two pressure drop curves coincide at equal flow rates of water and cyclohexane.

As the slug size analysis shows, the Y-junction dimensions have strong influence on the slug length and thus size for the same capillary dimensions. The pressure drop was also measured under the same operating condition and exhibited no effect of the Y-junction used for the same capillary. The results reveal the presence of a film, because in the absence of a film the pressure drop would be a strong function of the length of slug: a decrease in the length would enhance the capillary pressure and thus increase the overall pressure drop. However, the present study shows little effect of the slug size and only an influence of the flow ratio.

4.4.2.2. Theory—without film. In the previous sections, it has been conjectured that the organic liquid forms a wall film due to wetting properties of the two liquid phases and the capillary material. Since the film is probably only a few micrometer thick, it is virtually impossible to visualise it directly with the help of snapshots. We have therefore employed simplified models to provide evidence of the presence of a thin organic wall film. The experimental results are compared with theoretical pressure drops predicted by Eqs. (3) and (7) in Fig. 16. For Eq. (3), the theoretical pressure drop was calculated using the slug lengths and contact angles retrieved from the experimental snapshots. The contact angle was measured from the snapshot of static fluid. These values show reasonable agreement with the experimental results, although the discrepancy between the two increases with decreasing capillary diameter. In the experiments of Horvolgyi et al. [7] for very small capillaries (ID = 0.05 and 0.13 mm), it

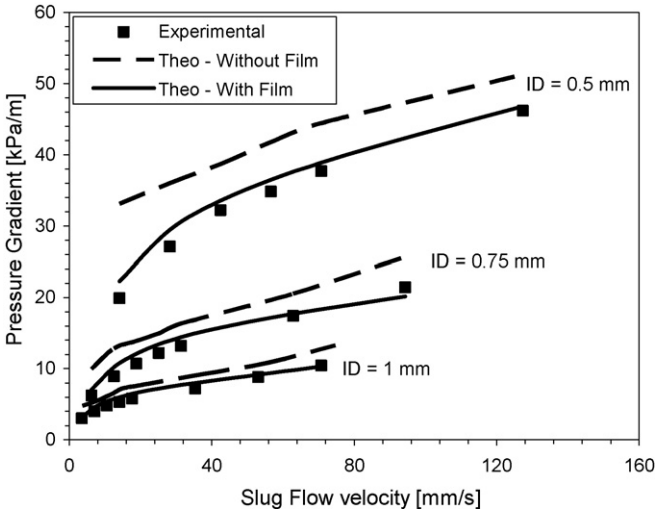

Fig. 16. Comparison of experimental pressure drop with predicated values at equal volumetric flow rates of water and cyclohexane.

was observed that this theoretical pressure drop under-predicts the overall pressure drop and this was explained as a result of the capillary pressure term not being suitable to describe the two phase capillary flow in a considerable section of the flow system.

In the present work, however, the analytical solution tends to over-predict of the pressure drop for all capillaries. This may well be due to the superior wetting properties of the organic phase on the capillary material, which results in the formation of a thin superficial film. This film provides a lubricating action on the embedded slug and yields annular flow behaviour exhibiting different pressure drop characteristics compared to the simplified model initially employed. Another possibility to explain the discrepancy is the internal circulations induced within each individual slug. When the slugs move through the capillary internal circulations arise within the slug, due to the shear between capillary wall and axis of the slugs, which reduces the thickness of the boundary layer and can eventually affect the capillary pressure. However, such circulations are of advantage in mass transfer because they enhance the diffusive penetration between two phases. It is thus important to implement the effect of film and internal circulations in the theoretical pressure drop calculations.

4.4.2.3. Theory—with wall film. Fig. 16 shows the comparison of theoretical pressure drop without and with film together with the experimental values at equal flow rate of both phases. The agreement between experimental and theoretical pressure drop with a wall film is reasonably good, especially in comparison to the model neglecting film formation. The film thickness calculated by Bretherton's law was in the range of 1–20 μm for all capillaries under the slug flow regime. Further model predictions at different Q_W/Q_{CH} flow ratio exhibit good agreement with the experimental values. The pressure gradient as a function of Q_W/Q_{CH} flow ratio is depicted in Fig. 17. As with the pressure gradient at equal flow rates, the results show good agreement with the experimental values at the low ratio values. For the larger capillary (ID = 1 mm), the agreement is good between Q_W/Q_{CH} equal to 0–2 for constant water flow and Q_W/Q_{CH} equal

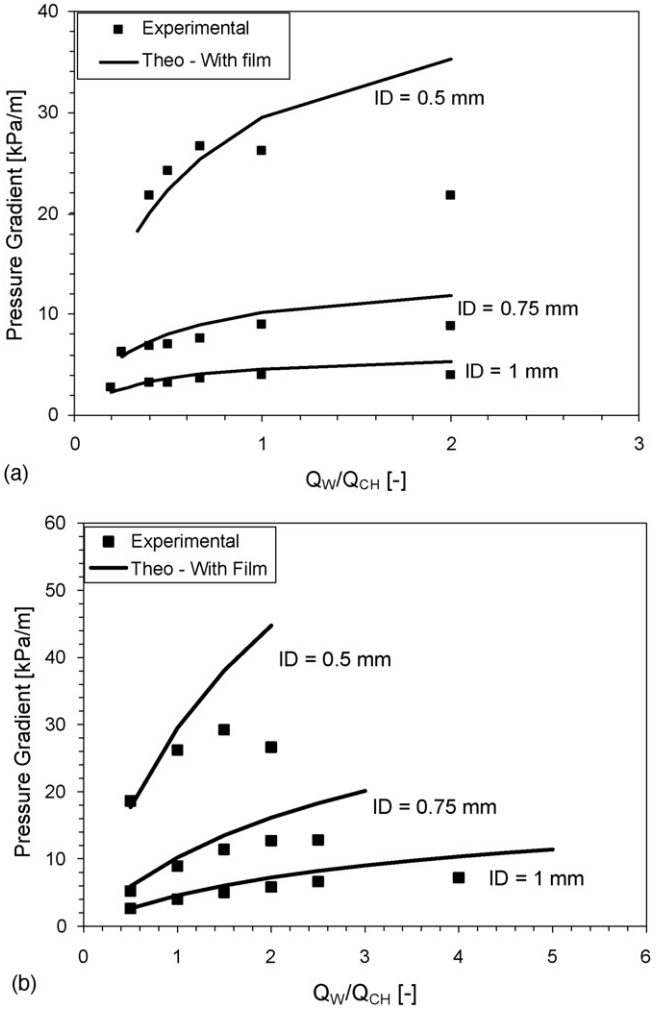

Fig. 17. Comparison of experimental and predicted pressure drops for unequal flow rates of water and cyclohexane. (a) Constant flow rate of water, 10 ml/h and (b) constant flow rate of cyclohexane, 10 ml/h.

to 0–4 for constant cyclohexane flow rate. However, the agreement between theoretical and predicted pressure drop worsens with decrease in the capillary diameter. For the small bore capillary (ID = 0.5 mm), it shows considerable deviation beyond a flow ratio 1 for constant flow rate of water and 1.5 for constant flow rate of cyclohexane. The disagreement between experimental and theoretical prediction at higher flow rates may be due to the transition of the slug flow regime into drop flow and deformed interface flow. Thus, the prediction of pressure drop with the wall film shows that its presence can significantly alter pressure drop while the measurements of pressure drop along the capillary microreactor corroborates the presence of such a film.

4.4.3. Power input

Power input, an interesting parameter for benchmarking technical reactors, has been calculated from the pressure loss due to the Y-junction in the capillary microreactor. The results obtained were compared with various liquid–liquid contactors given in Ref. [11] as shown in Table 2. The comparison shows that the liquid–liquid slug flow capillary microreactor requires much less

Table 2
Power input requirement for various liquid–liquid contactors

Contactor type	Power input (kJ/m^3 of liquid)
Agitated extraction column	0.5–190
Mixer-settler	150–250
Rotating disk impinging streams contactor	175–250
Impinging streams	280
Impinging stream extractor	35–1500
Centrifugal extractor	850–2600
Liquid–liquid slug flow (present work)	0.2–20

power than the alternatives to provide such a large interfacial area.

5. Conclusion

Experiments were carried out to investigate flow regime, slug size, interfacial area, pressure drop and power requirement under various operating conditions using different Y-junction mixing elements with various downstream capillaries. The capillary and Y-junction dimensions show a significant effect on slug size and thus interfacial area, which increases with decreasing dimensions. The pressure drop was measured across the Y-junction and along the length of slug flow capillary. A theoretical prediction for pressure drop along slug flow capillary was developed based on the capillary pressure and hydrodynamics pressure drop without a wall film and compared with experimental results. The discrepancies observed with this theory and the underlying reasons were identified. The presence of an organic wall film was one of the reasons and an improved model taking it into consideration showed good agreement with the experimental values. The power input was calculated using the pressure losses over the mixing element and it was found that slug flow capillary microreactor is superior to conventional equipment in the sense of providing more interfacial area with less power. In addition to this, precise tuning of interfacial area and thus mass transfer across the interface is possible in this reactor as a result of the well-defined flow patterns. These experimental findings will be helpful in devising a more detailed computational model for predicting the mass, heat transfer and reaction kinetics in liquid–liquid slug flow capillary microreactor. Future work will be devoted to developing such a model with the objective of predicting the mass transfer rates from first principles.

Acknowledgement

The authors acknowledge the assistance of Mr. Yogesh M. Harshe in performing the experiments described.

References

[1] J.R. Burns, C. Ramshaw, The intensification of rapid reactions in multiphase systems using slug flow in capillaries, Lab Chip 1 (2001) 10–15.
[2] G. Dummann, U. Quittmann, L. Groschel, W. Agar David, O. Worz, K. Morgenschweis, The capillary-microreactor: a new reactor concept for the intensification of heat and mass transfer in liquid–liquid reactions, Catal. Today 79–80 (2003) 433–439.
[3] M.N. Kashid, I. Garlach, J. Franzke, J.F. Acker, F. Platte, D.W. Agar, S. Turek, Internal circulation within the liquid slugs of liquid–liquid slug flow capillary microreactor, Ind. Eng. Chem. Res. 44 (2005) 5003–5010.
[4] A. Kawahara, P.M.Y. Chung, M. Kawaji, Investigation of two-phase flow pattern, void fraction and pressure drop in a microchannel, Int. J. Multiphase Flow 28 (2002) 1411–1435.
[5] K. Michiel, Hydrodynamics of Taylor Flows in Capillaries and Monolith Reactors, Ph.D. Thesis, Delft University Press, Netherlands, 2003.
[6] Z.M. Zorin, N.V. Churaev, Immiscible liquid–liquid displacement in thin quartz capillaries, Adv. Colloid Interface Sci. 40 (1992) 85–102.
[7] Z. Horvolgyi, E. Kiss, P. Janos, Experimental studies on the control of slug flow by interfacial forces in silylated capillaries, Colloids Surf. 55 (1991) 257–270.
[8] M.E. Charles, The pipeline flow of capsules (Part 2), Can. J. Chem. Eng. (April) (1963) 46–51.
[9] J. Bico, D. Quere, Liquid trains in a tube, Europhys. Lett. 51 (2000) 546–550.
[10] M.N. Kashid, F. Platte, D.W. Agar, S. Turek, Computational modelling of slug flow in capillary microreactor, J. Comput. Appl. Math., in press.
[11] A.M. Dehkordi, Novel type of impinging streams contactor for liquid–liquid extraction, Ind. Eng. Chem. Res. 40 (2001) 681–688.